JOURNAL OF MATERIALS SCIENCE 10 (1975) 41–51

Axial compression fracture in carbon fibres

H. M. HAWTHORNE, E. TEGHTSOONIAN
Centre for Materials Research, The University of British Columbia, Vancouver 8, British Columbia, Canada

Axial compression fracture of carbon fibres was studied by embedding single fibres in epoxy resin and compressing the specimens parallel to the fibre axis. By careful optical monitoring of the fibre surface the earliest stages of fracture were identified leading to estimates of the fibre axial compression failure strengths. Compression strength decreases markedly from about 2.2 GN m^{-2} for moderately oriented fibres to < 1 GN m^{-2} for highest modulus filaments. The trend towards decreasing compression strength with increasing anisotropy is explained on the basis of an increasing fibre microfibrillar nature. However fracture morphology studies show that the unduly rapid strength decrease results from an increasing degree of fibre outer layer ordering which accompanies increasing axial anisotropy in carbon fibres since cracking occurs first on the more highly aligned filament surfaces. It is suggested that fibre compression fracture changes from a shear to a micro-buckling or kinking mode with increasing fibre anisotropy, where the latter initiates in individual, well-aligned but uncoupled microfibrils. The similarity of fine axial compression fractures in oriented carbon fibres to those found in elastica loop experiments is noted as are the possible implications which the low strain-to-failure in compression of very high modulus fibres might have for practical composites.

1. Introduction

In a recent paper [1] we reported on some earlier experiments with single-fibre model composites designed to induce interface failure between the matrix and large diameter pitch-based carbon fibres embedded in the epoxy resin. However it was found that upon compressing the curved-neck samples parallel to the fibre axis, compression-induced shear failure of the filaments usually occurred first and precluded any debond such as is obtained in similar tests with glass and boron fibres [2]. These fibre failures were sufficiently gross to disrupt the interface and surrounding resin to allow their ready visual detection. Apparently similar gross shear fractures in PAN and rayon-based fibres have also been noted by us [1] and other workers [3, 4].

Approximate estimates of compression strains adjacent to the filament fractures (in the varying-section resin specimens) suggested a progression in fibre strain-to-failure from about 2.5% to below 1% as the carbon fibre modulus increased. However subsequent examination of these specimens under higher magnification revealed the presence of fine circumferential cracks on some fibres which suggests that fracture initiates at lower strains than those corresponding to the interface-disrupting filament shear failures.

In the present paper we report the results of a more detailed investigation of the axial compression-induced failure of embedded carbon fibres of various types and Young's modulus. The term carbon fibre is used to denote all fibres irrespective of microstructure or process history.

2. Experimental

2.1. Sample preparation

Pitch-based carbon fibres which had been stretch-graphitized to varying extents at $\sim 2750°C$ and a few commercial carbon fibres were embedded in epoxy resin (EPON 828/10 p.h.r. TETA) by glueing across an aluminium split mould as illustrated in Fig. 1a. After curing for 16 h in the mould at room temperature the resin block was removed and top and bottom surfaces milled flat and parallel. The milled

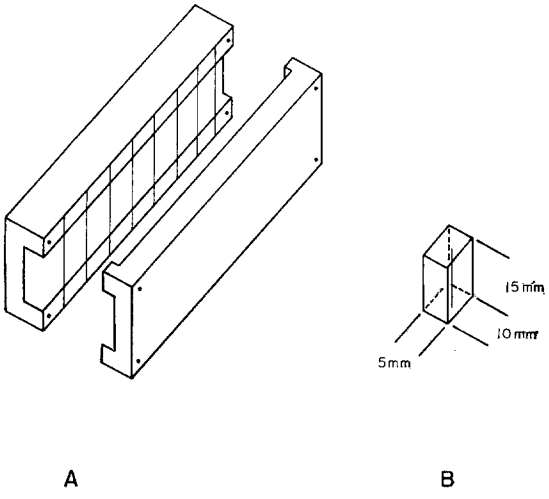

Figure 1 (a) Aluminium split mould. (b) Single fibre compression test specimen.

surfaces were then lightly polished to ensure that fibre ends were co-planar with the surfaces. Individual specimens were cut, ground and polished to give final sample dimensions close to that of Fig. 1b. Fibres were perpendicular to the end surfaces and about 2 mm from one side to facilitate subsequent microscopic examination. Samples in which embedded fibres were poorly aligned or otherwise unsuitable for testing were discarded. The residual strain on some embedded fibres due to resin cure shrinkage was measured directly using markers which were either fibre defects or small lengths of fine (Thornel 75) fibre glued across the test fibre prior to moulding.

2.2. Testing

Samples were compressed between parallel anvils on an Instron testing machine at 0.02 in min^{-1} crosshead speed and using a compression load cell. Specimen strains were measured from the load-displacement plot. Comparison of the strains thus measured was made on several 2 cm long samples with those determined using a half inch strain-gauge extensometer and also with the corresponding actual fibre strains measured between markers using a travelling telescope. Initial testing of a few samples determined approximate failure strain for a particular fibre modulus. Thereafter samples were loaded incrementally, followed, after each successive loading, by removal from the machine and examination of the fibre for failures. Through the resin these were best detected with reflected polarized light using an optical microscope with long focus objectives and a high intensity light source at 100× to 200× magnification. Compression strain increments of about 0.1% were applied until evidence of filament fracture was first observed and the failure strain was taken as the mean of the last two strain values.

3. Results

In testing pitch-based carbon fibres fine compression-induced cracks were directly observed to occur on all but the lowest modulus fibres. A photograph of such cracks, taken through ~ 0.5 mm of resin, is shown in Fig. 2. For highest modulus fibres many cracks appeared simultaneously and fairly evenly distributed along the fibre whereas with lowest modulus filaments usually only one failure was apparent. Further loading of a sample subsequent to fibre cracking produced a gradual coarsening of the cracks until eventually one or more developed into a distinct shear of the fibre ends past each other. The start of this shearing stage of failure was where the interface and the surrounding resin became disturbed as described previously [1].

The difference in strain between that at which initial fibre cracking occurred and that corresponding to the more gross shear failure was greatest for the high modulus filaments. For the lowest modulus fibres ($E \sim 130$ GN m^{-2}) it was often not possible to detect the fine cracking before observing the beginning of a sheared fracture, which was thus often the earliest

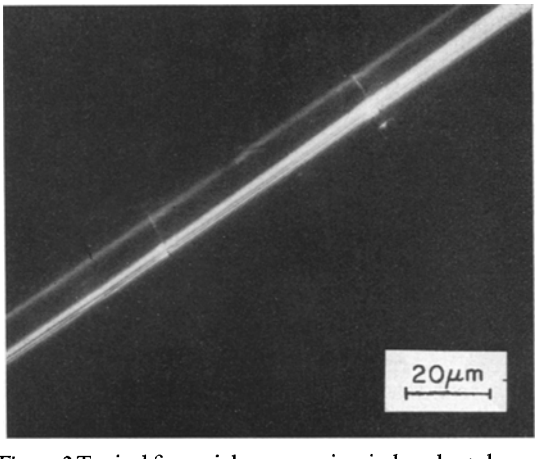

Figure 2 Typical fine axial compression-induced cracks on surface of pitch-based carbon fibre ($E \sim 390$ GN m^{-2}); taken through ~ 0.5 mm resin using reflected polarized light.

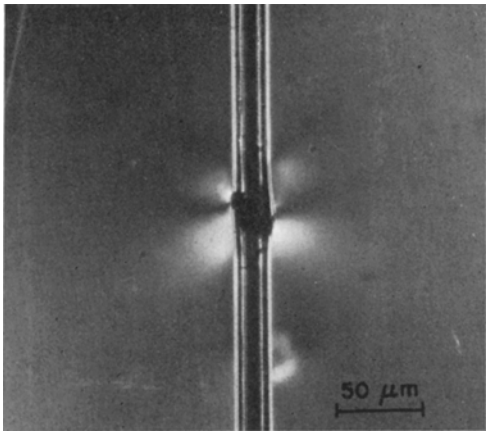

Figure 3 Early stage compression-induced shear fracture in low modulus (E ~ 130 GN m^{-2}) carbon fibre; taken as for Fig. 2 but with additional illumination projected in at both sides to show fracture more clearly.

indication of failure for these fibres. An example of such a fracture is illustrated in Fig. 3. That fine cracking did occur sometimes even in these low modulus fibres prior to gross failure was inferred from several observations of a separation of fibre ends inside the specimen as shown in Fig. 4. This probably initiated from a compression crack which upon unloading the sample after compression produced a tensile separation of the fibre ends from the fracture by sliding along a length of debonded interface.

Although much more difficult to observe clearly on fibres prepared from PAN and rayon precursors because of their irregular surfaces and small diameter, fine compression-induced cracks or fractures were produced on PAN I and Thornel fibres as shown in Fig. 5.

The experimental results for the compression tests on all fibres are presented in Table I, column 3. The failure strains are those measured from the load-deflection curves. For the pitch-based fibres Young's modulus values are the averages determined for each group of fibres which had been stretch-graphitized to different extents [5]. Those for PAN and Thornel fibres were from source data. All of the Thornel 75 fibres and one high modulus pitch-based fibre

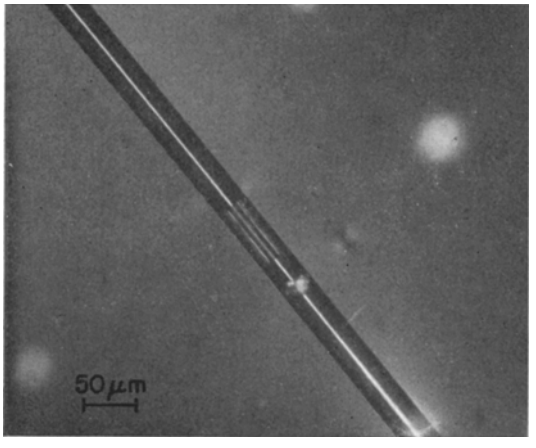

Figure 5 Fine axial compression-induced transverse cracking on Thornel 50 (a) and Pan I (b) carbon fibres; polarized light through resin as before.

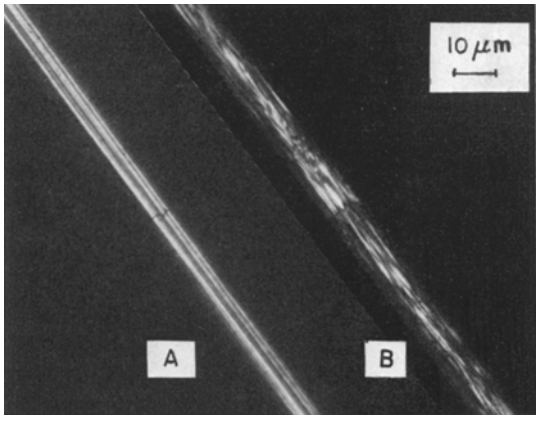

Figure 4 Tensile separation of fibre ends away from a fine transverse compression crack after unloading the specimen. Low modulus fibre (E ~ 130 GN m^{-2}); polarized light; through ~ 1 mm resin.

were found to be cracked upon moulding indicating that fibres sustained some compression strain due to resin shrinkage on curing.

To obtain the actual compression strain existing in the fibre at fracture (column 5, Table I) corrections were made to the experimental data (column 3) which take into account (a) the relation of sample strain, which could only be measured approximately from load-elongation plots for the short-length specimens, to true specimen strain and (b) the residual fibre strain existing in the split-mould specimens. Extensometer-measured strains on slightly longer but otherwise similar specimens indicated machine-measured strains were too large by about 15%. A few direct measurements, during compression of specimens containing marked fibres gave strain values ~ 8% lower than those obtained from crosshead displacement. Con-

TABLE I Measured compression test results and derived total fibre compression strains at failure

Mean fibre modulus (GN m^{-2})	Number of tests	Average measured compression test strain at fibre failure (%) A	Corrected average test strain (%) B = 0.9 A	Total fibre compression strain at failure (%) C = B + 0.15
131	17	1.68 ± 0.33	1.51 ± 0.33	1.66 ± 0.33
190	9	1.20 ± 0.19	1.08 ± 0.19	1.23 ± 0.19
262	11	0.85 ± 0.18	0.76 ± 0.18	0.91 ± 0.18
330	26	0.63 ± 0.18	0.57 ± 0.18	0.72 ± 0.18
393	16	0.36 ± 0.09	0.32 ± 0.09	0.47 ± 0.09
450	6	0.16 ± 0.12	0.14 ± 0.12	0.29 ± 0.12
258 (Thornel 40)	8	0.63 ± 0.1	0.57 ± 0.1	0.73 ± 0.1
355 (Thornel 50)	6	0.56 ± 0.13	0.50 ± 0.13	0.65 ± 0.13
530 (Thornel 75)	8	0	0	⩽ 0.15
345 (PAN I*)	2	0.5	0.45	~ 0.6

*Harwell Fibres.

sequently the average test data of column 3 are reduced by 10% as in column 4, Table I.

Listed in Table II are assessments of the residual strain incurred by marked fibres when moulded in the split-mould and more accurate measurements from those moulded in long single moulds. In the latter, single fibres were glued to the top of the mould only to allow greater fibre

TABLE II Fibre residual and test compression strains for specimens containing fibres with markers

Mean fibre modulus (GN m^{-2})	Residual fibre compression strain on moulding (%) A*	Compression test fibre failure strain (%) B	Total fibre strain at Failure (%) A + B	Mean A + B (%)
	~0.3	1.70	2.0	
131	~0	~1.8	~1.8	1.88
	0.35	1.49	1.84	
	0.27	1.23	1.50	
	0.15	1.10	1.25	
	0.15	0.98	1.13	
190	0.50	0.78	1.28	1.30
	0.5	0.64	1.14	
	0.5	0.76	1.26	
	~0.1	1.41	1.51	
262	~0.2	0.76	0.96	0.96
	~0.05	0.70	0.75	
	~0.2	0.76	0.96	
	0.23	0.51	0.74	
330	0.23	~0.56	0.79	0.78
	~0.1	0.55	0.65	
	~0.1	0.63	0.73	
	0.2	0.64	0.86	
355 (Thornel 50)	~0.2	~0.4	~0.6	~0.6
	0.44	Already cracked	⩽0.44	
393	~0.1	0.48	0.58	~0.5
	~0.2	0.34	0.54	

*Values marked thus ~ are from split mould specimens, others from moulding of less restrained fibres in long tube moulds.

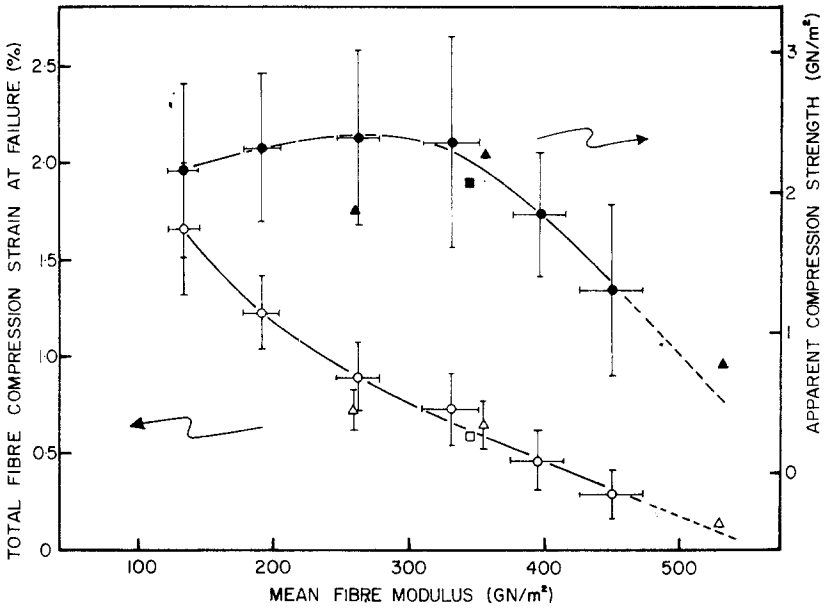

Figure 6 Variation of total axial compression strain-at-fracture data for all fibres (from Table II) and corresponding fibre compression strengths (assuming $E_{\text{compression}} \equiv E_{\text{tension}}$) with fibre Young's modulus. Error bars represent standard deviations. Circles: pitch-based fibres; triangles: rayon-based fibres; squares: PAN-based fibres.

contraction on resin cure. Also listed in Table II are the failure strains (crosshead deflection) for all these marked fibre specimens. Average total failure strains for each fibre group (Table II, column 5) when compared with the mean data of the main compression tests on split-mould specimens (column 3, Table I) suggest that a value of $\sim 0.15\%$ is the best estimate of the mean residual fibre strain incurred by the filaments when moulded in the split-mould. This strain is therefore added to the data of Table I, column 4 to give the mean total fibre compression strain-at-failure for each fibre group as in Table I, column 5. The final result for Thornel 75 fibres is a maximum value since it is not known at what strain they actually cracked.

Total fibre axial compression strain-at-fibre-fracture data for all filaments are plotted against fibre modulus in Fig. 6. The relatively larger spread of results for the lowest modulus fibres probably reflects the use of the two indicators of early fibre compression failure as mentioned above.

4. Discussion

4.1. Fibre axial compression strengths

An assessment of the effect of the approximations inherent in both the fibre residual strain estimate and in obtaining the precise fibre strain-at-fracture on the strain data of Fig. 6 is of interest. Even if the 10% fibre strain correction is in error by several percent (say $\pm$ 3%) and the estimated average mould strain is wrong by 0.05% strain ($\pm$ 33% of estimate) the maximum deviation from present results would range from $\pm$ 7% to $\pm$ 18% (with increasing filament modulus). Since this is within the experimental error we are confident that the data of Fig. 6 reasonably represents the true mean fibre strains at the onset of filament compression failure for each modulus group. A fairly regular progression in fracture strain for all the carbon fibres, is obtained, consistent with the approximate values calculated from the previous "debond" experiments [1] as described in the Introduction but at somewhat lower strains.

However fibre axial compression strengths, calculated from the failure strain and mean Young's modulus, assuming the latter is the same in compression as in tension, apparently indicate a different trend. As shown in Fig. 6 with increasing modulus fibre compression strengths do not vary much up to moderate modulus values but thereafter they decrease to quite low values.

Because of the experimental difficulties of

ensuring satisfactory mounting and moulding of individual, thin commercial fibres and with detection of fine cracking on their surfaces the limited data for these filaments are less certain than those of the larger, smooth-surfaced, pitch-based fibres. Nevertheless, except for the Thornel 40 specimens, their estimated compression strengths lie reasonably close to the general trend of the pitch-based fibre data. The compression strength of PAN type II and type A fibres could not be obtained as fibre fracture was not observed before the epoxy resin samples failed in shear at $\sim 3\%$ strain.

The only known information in the literature concerning carbon fibre axial compression strength measurements with which to compare present data are estimates for the strength of Thornel 25 and Thornel 40 fibres [3]. Based on an indirect assessment of the Poisson contraction during tensile loading of epoxy resin specimens containing a fibre embedded transverse to the loading direction, average values of ~ 1.5 GN m^{-2} and ~ 2.5 GN m^{-2} were obtained for Thornel 25 and 40 respectively. Although detected as sheared fibre failures [3], nevertheless these compression strengths show some measure of agreement with present results. Also their relative strength tends to support the slight indication from the pitch-based fibre results of a maximum in the strength versus modulus curve.

Fine fibre cracks have also been observed on the compression side of the loop tip in elastica loop bending experiments on PAN [10] and both pitch and rayon-based carbon fibres [7]. We shall discuss this more fully in a subsequent paper [7], but note here that the fibre strain-to-fracture data in the present axial compression tests are about the same as the strains existing in the loop tip at which such cracking occurs in corresponding fibres.

The compression test results are in marked contrast to those of both rayon [6] and pitch-based [5, 7] fibres in tensile testing where strength increases with modulus. Only in some PAN-based fibres, e.g. those prepared from Courtelle precursor, has a tensile strength decrease with increasing filament Young's modulus been observed [8]. Also in contrast to the situation with tensile failure of carbon fibres from all three precursors [5-7, 9], axial compression fracture does not seem to be associated with gross fibre flaws. The examination of numerous compression microcrack fractures both by isolation of fibre ends from the matrix and by progressive polishing through fibre longitudinal sections has revealed only a few examples where the crack might possibly have been associated with an observable flaw.

The overall shape of the experimental fibre compression strength curve can be explained qualitatively as follows. On the basis of brittle fracture theory the compression strength of an isotropic glassy carbon would be expected to approximate to its intrinsic (flaw-free) strength. Extrapolation of the present compression results curve to the isotropic fibre modulus (~ 30 GN m^{-2}) suggests that a strength between 1.5 and 2.0 GN m^{-2} might be appropriate. This is reasonable in view of the tensile strength results reported for similarly heat-treated, isotropic, pitch-based [5] and rayon-based fibres [6] of ~ 0.7 GM m^{-2} since flaw-free strengths are approached in tension only at much smaller gauge lengths than those used in normal tensile tests [10, 11]. Also relevant is a calculated value for the intrinsic strength of an isotropic PAN-based fibre at 1.55 GN m^{-2} [12] even though this would probably be more relevant to fibres of lower heat-treatment temperature. Alternatively, if a microplastic failure criterion is considered for the isotropic carbon fibres the same curve extrapolation gives a "plastic yield strength" value similarly related to the corresponding material indentation hardness [7] as for other glassy solids [13]. Thus reasonable extrapolation of present compression strength data would be consistent with the anticipated strength of isotropic, glassy carbon fibres (heated $> 2500°C$) whichever viewpoint is taken, but we prefer the former at this stage.

As fibre Young's modulus increases from the isotropic value so the carbon fibre intrinsic tensile strength increases [7, 12]. Filament compression strength might therefore be expected to increase also. However because of the unique microstructural features of the anisotropic carbon fibres it is probable that axial strength in compression will deviate from intrinsic strengths progressively more markedly, with increasing modulus. In such fibres, composed of wrinkled and entangled ribbons of turbostratic graphite layers mutually separated by microvoids, these microfibrils are progressively more highly aligned along the fibre axis and tend towards a more "graphitic" nature (in terms of crystallite size and perfection) the higher the Young's modulus [5, 14]. An increasing radial ordering and decreasing transverse interfibrillar coupling

usually also accompanies an increasing axial preferred alignment in carbon fibres [14, 15]. For very high modulus fibres, therefore, a decreasing compressive strength is likely considering that in the limit of perfect axial alignment and minimum lateral microstructural interactions, fibre axial compression behaviour will probably approach the weak strength of crystalline graphite in the *a*-direction. Consequently the resultant filament compression failure strengths may first increase with growing fibre anisotropy from the isotropic material intrinsic strength value and then decrease as modulus approaches very high values. This is reasonably consistent with the present experimental results except that the strength decrease with increasing modulus is somewhat steeper and perhaps begins earlier than might be anticipated. Thus extrapolation of the strength curve of Fig. 6 would suggest that fibres of Young's modulus ~ 600 GN m^{-2} have essentially zero compression strength which is absurd and requires explanation.

4.2. Compression crack morphology

To learn something of the nature of axial compression fractures in carbon fibres we sought initially to isolate the filaments from the matrix and to observe directly the locus of failure on separated fibre ends. Since it was not possible to dissolve away even the thinnest over-layer of cured epoxy resin sufficiently to remove fibres without damaging them some representative fibres were moulded in a readily soluble, clear acrylic resin. However, because of the large cure shrinkage of this resin all fibres were cracked and even sheared on moulding, the high modulus ones being most severely fractured. As shown in Fig. 7 separated fracture surfaces from typical axial compression failures (cf. Fig. 3) for lowest modulus fibres exhibit both rough and smooth areas and contain some crushed debris. Similarly sheared fracture surfaces from higher modulus fibres tend towards a more serrated texture and sometimes contain small platelet-like protrusions.

To investigate fracture profiles in fibres which had only sustained compression strains sufficient to produce the fine cracks seen on the fibre surface as per Figs. 2 or 5, successive polishing of specimens through longitudinal sections of the embedded carbon fibres was used. For the majority of fibres the compression crack retained its hair-like appearance and the same general

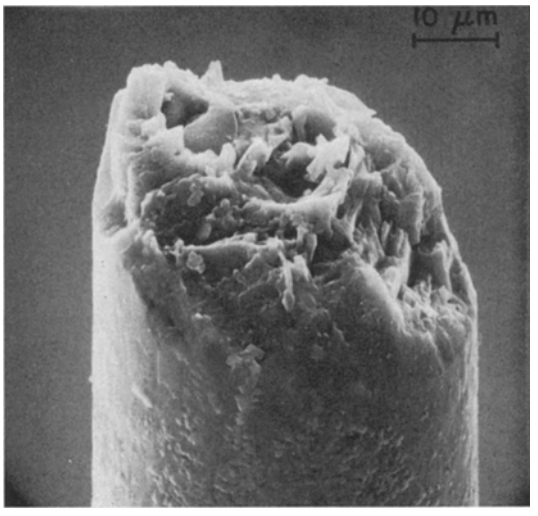

Figure 7 Scanning electron micrograph of an early stage, axial compression-fractured surface of a low modulus ($E \sim 130$ GN m^{-2}), pitch-based, carbon fibre. Isolated from a soluble acrylic matrix.

aspect throughout. The cracks mostly had a curved profile, as shown in Fig. 8, with the degree of curvature often changing across the fibre section. Occasionally in fibres containing multiple cracks a sequence of double crack profiles was revealed which indicated a biconical or "hourglass" type of failure locus, somewhat analogous to the shear-induced compression failures characteristic of some brittle granular materials [16].

Scanning electron microscope (SEM) examination of the polished fibre sections confirmed

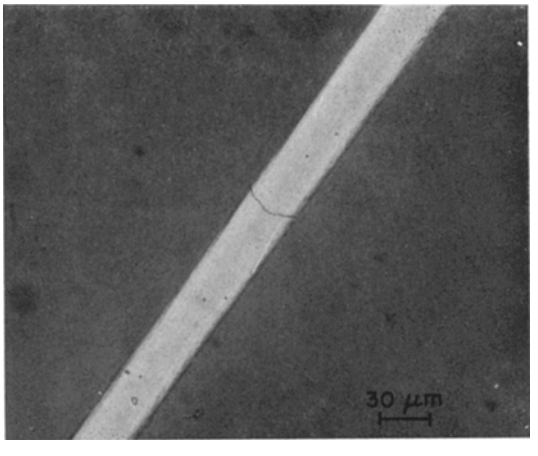

Figure 8 Typical reflected polarized light optical micrograph of a polished longitudinal section of a fine-cracked, pitch-based carbon fibre ($E \sim 260$ GN m^{-2}).

that the compression fractures are indeed very narrow line cracks and fibres polished to their mid-section exhibit very small discontinuities or offsets at the fibre edge. In this respect there is some similarity to the crack-like features observed on the compressive side of carbon fibres bent in elastica loop experiments [7, 10].

Partial cracks were sometimes observed on polished fibre longitudinal sections, as in Fig. 9,

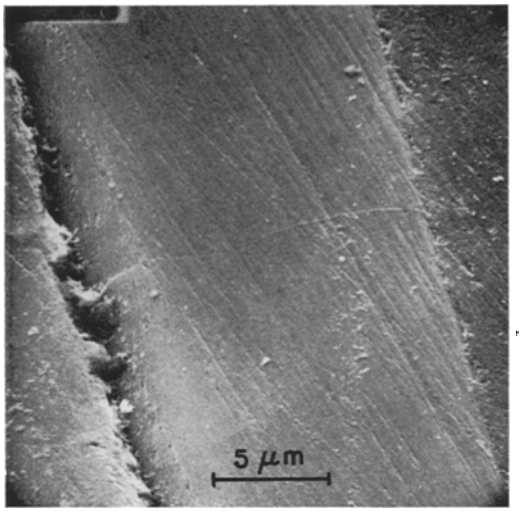

Figure 9 Scanning electron micrograph of a lightly polished section of an early stage, axial compression-cracked high modulus carbon fibre ($E \sim 390$ GN m^{-2}). Crack fades out in centre of fibre.

which suggested a gradation in the severity of fracture from surface to core. That cracking invariably occurs first in the outer layers of high modulus carbon fibres in the early stages of compression failure was subsequently established by examination of many such cracked fibres before and after slight polishing into their sections. Thus Fig. 10 shows high magnification polarized light micrographs of the same area of an embedded high modulus fibre. The polished section width in Fig. 10b, at $\sim 2/3$ the fibre diameter, indicates that after removal of only 1/8 of the fibre thickness no trace remains of the multiple compression cracks which were clearly visible on the fibre surface (under a thin overlayer of resin) in Fig. 10a.

The finding that axial compression fracture first initiates in the peripheral regions of oriented carbon fibres is entirely consistent with the well established fact that practically all carbon fibres exhibit a more axially aligned basal-plane texture and more graphitic outer surface layer compared with the fibre core [1, 14, 17]. This sheath becomes more evident the higher the fibre average degree of axial preferred orientation and, being of higher Young's modulus than the core, it will bear a progressively greater proportion of any fibre stress for a given compression strain and so might be expected to fail prior to complete fibre fracture.

The filament radial structural heterogeneity provides an explanation for the experimental strength reductions discussed above. During specimen testing the fibre compression strains at fracture of their surfaces were being monitored. The compression strengths of Fig. 6, calculated

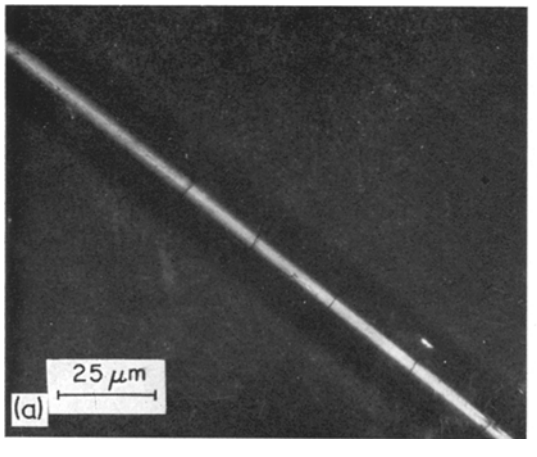

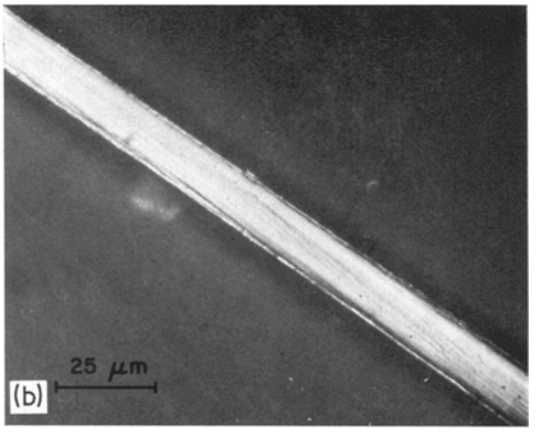

Figure 10 (a) High magnification polarized light optical micrograph, taken through a thin resin layer, of a multiple-cracked, high-modulus carbon fibre ($E \sim 440$ GN m^{-2}). (b) Same area of fibre as (a) after very lightly polishing away $\sim \frac{1}{8}$ of the fibre thickness.

from the average fibre Young's modulus rather than the more appropriate higher modulus of the outer layers, are therefore too low. The effect of this will be progressively greater the higher the average fibre modulus and thus will contribute increasingly to the strength reduction. Also related to this fibre microstructure and similarly effective in lowering the measured strength results is the existence of an inherent fibre surface compression strain, axial as well as radial, arising from differences in thermal contraction between sheath and core on cooling the fibres from their high processing temperatures [15]. We consider that the operation of both these factors is sufficient to explain the otherwise unexpectedly severe drop-off in compression strengths for the more oriented carbon fibres.

4.3. Mechanism of compression fracture

From present and earlier experiments [1] there seems to be a trend in the nature of compression fracture in embedded carbon fibres of different microstructure. As fibre anisotropy increases the tendency is away from a single catastrophic shear-like failure to what is often a series of fine, partial microcracks. This variation in failure character is further exemplified by comparison of the typical fracture surface of an early stage compression failure of a low modulus fibre (Fig. 7) with that from a microcracked high modulus pitch-based fibre in Fig. 11. (The latter was exposed when, upon polishing not quite parallel to its axis, through a cracked fibre past its mid-section, the tapered fibre end was pulled back from the crack and lifted out of the shallow resin trough). The remaining portion of the crack face shows clearly a very different topography from that of Fig. 7. The fine scale texture, of the order of ~ 0.1 μm, on the fracture surface is similar to that previously observed on transverse sections of oriented pitch-based fibres [5] and on transverse fracture surfaces of similar rayon-based fibres [18] and may be evidence for large fibrils in the fibre microstructure [14]. In any case the fracture here takes place essentially on a plane perpendicular to the fibre (and compression) axis and has generally similar features to that observed on the compression side of the fractured end of a PAN-based fibre broken in loop bending experiments which was considered due to a buckling failure [10].

A shear failure mechanism seems appropriate for the more isotropic fibres. If carbon fibres can be considered as an aggregate of turbostratic graphite crystallites the trend in compression strength results could be explained on the basis of a crystallite shear strain criterion, somewhat analogous to that proposed recently for tensile failure in such fibres [12]. Thus a critical stress for fibre shear failure in compression (σ_c) is defined as:

$$\sigma_c = \tau_c / \sin\phi \cos\phi$$

where ϕ is the mean angle between basal planes and the fibre axis and τ_c is the critical resolved shear stress for the crystallites. τ_c is related to the crystallite shear strain failure criterion γ_c by:

$$\tau_c = \gamma_c c_{44}$$

where c_{44} is the pertinent shear modulus. The variation of fibre compression strength with modulus could result from the competing contributions of an increasing basal plane preferred orientation about the fibre axis, tending to increase strength, and a proposed decreasing microscopic shear modulus for more ordered crystallites (especially on the fibre outer layers), tending to diminish fibre strength. However considerable reductions in c_{44} would be required to obtain correspondence with the experimental results for the high modulus fibres.

In view of the changing appearance of fibre compression fractures and because of the peculiar microfibrillar structure of carbon filaments we suggest that it is perhaps more

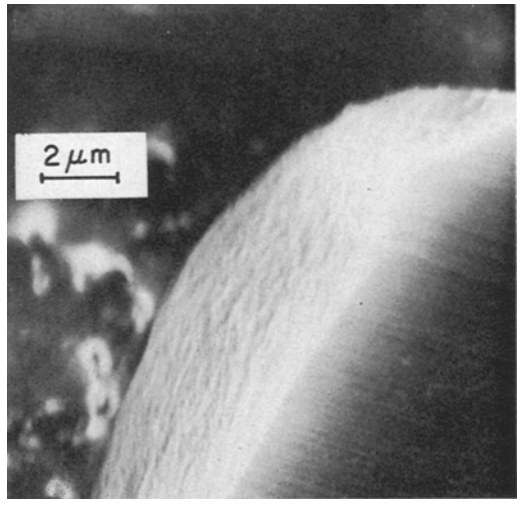

Figure 11 Scanning electron micrograph of the edge of an early stage, axial compression-cracked surface of a high modulus ($E \sim 330$ GN m^{-2}) pitch-based carbon fibre. Fracture surface exposed on thin section ($\sim \frac{1}{6}$ diameter) when adjacent piece lifted away on polishing.

appropriate to discuss the axial compression failure of oriented carbon fibres in terms of a buckling or kinking structural instability somewhat analogous to inhomogeneous compression behaviour in some other anisotropic materials. During compression of wood parallel to the grain macroscopic failure follows from a buckling distortion of those cellular wood fibrils which are both aligned nearly parallel to the load axis and low in interfibrillar lateral cohesion [19]. In the case of hcp metals such as Zn or Cd a kinking deformation occurs when single crystals are compressed parallel to their basal planes [20]. Such kinking also occurs in pyrolytic graphite [21]. Thus in axial compression of highly oriented carbon fibres microcracking may initiate as a buckling or kinking of single microfibrils of well-ordered layer packets which, because they are less interwoven and coupled with their neighbours than those of lower modulus fibres, would be less constrained to deform individually. This localized distortion, which need not involve dislocations but rather "crystallite regions weak in shear" would probably occur preferentially along lengths of transversely unsupported microfibrils adjacent to large voids or axial cracks which arise from cooling down from high processing temperatures [15]. Even on moderately oriented fibres these considerations would be expected to apply to the more highly aligned fibre outer sheaths.

From present evidence it is considered that simple shear initiation of axial compression failure in glassy carbon fibres progressively changes to the microbuckling mode as fibre anisotropy increases. Further information on failure mechanisms may arise from studying the effects which boron doping or neutron-irradiation may have on filament compression strengths since these are known to significantly alter the structure and other properties of carbon fibres [22].

4.4 Possible implications for composites

The post-gelation shrinkage in the room-temperature curing resin system used to prepare the single fibre-resin specimens was sufficient to cause multiple axial compression fracture in carbon fibres of modulus $\gtrsim 450$ GN m^{-2} when moulded as per Fig. 1. Whether such cracking can occur in fabricating real composites of high modulus fibres and elevated temperature-cured resins will depend on the degree of restraint on the resin linear cure shrinkage imposed by the large volume of fibres and on the extent of axial residual stresses due to mismatch of thermal expansivity between fibre and resin. If compression microcracking were to occur in practice on very high modulus carbon fibres, even only on the filament outer layers, then the efficiency of translation of fibre properties into the composite would undoubtedly be impaired. It seems likely also that the propensity to low strain axial compression fracture of very high modulus carbon fibres would have a significant influence on the compression failure behaviour of unidirectional composites fabricated therefrom.

5. Conclusions

The conclusions from this work can be summarized as follows:

(a) It has been shown that axial compression fracture of carbon fibres can be studied successfully by supporting single fibres in epoxy resin specimens and compressing these parallel to the fibre direction.

(b) By carefully monitoring the fibre surfaces in the resin using high magnification optical microscopy the earliest stages of fibre fracture can be identified and can provide a good estimate of the fibre compression failure strengths.

(c) The apparent axial compression strengths of carbon fibres do not vary much with filament modulus up to moderate orientations; thereafter strengths decrease markedly with increasing fibre anisotropy.

(d) In highest modulus fibres axial compression cracking occurs initially in the fibre outer layers.

(e) The axial compression failure of carbon fibres is due to either a shear or buckling mechanism and the overall fracture behaviour can be adequately explained on the basis of the known fibre microstructural features.

Acknowledgements

We express our thanks to Mr G. Fraser for assistance with the experimental work and gratefully acknowledge the financial support of the Defence Research Board of Canada.

References

1. H. M. HAWTHORNE and E. TEGHTSOONIAN, Symposium on "Interfacial Bonding and Fracture in Polymeric, Metallic and Ceramic Composites" Paper 4, U.C.L.A., November 1972. Also *J. Adhesion* **6** (1974) 85.

2. L. J. BROUTMAN, "Interfaces in Composites", *A.S.T.M. S.T.P.* **452** (1969) 27.
3. J. B. KOENEMAN, Ph.D. Thesis, Case Western Reserve University, Cleveland, 1970.
4. B. HARRIS, P. W. R. BEAUMONT and E. M. DE FERRAN, *J. Mater. Sci.* **6** (1971) 238.
5. H. M. HAWTHORNE, Proc. 1st International Carbon Fibres Conference, London, 1971 (Plastics and Polymers Conference Supplement Section 5) p. 81.
6. R. BACON and W. A. SCHALAMON, Applied Polymer Symposia Section 9 (1969) 285.
7. H. M. HAWTHORNE, to be published.
8. R. MORETON, W. WATT and W. JOHNSON, *Nature* **213** (1967) 690.
9. J. W. JOHNSON, Applied Polymer Symposia Section 9 (1969) 229.
10. W. R. JONES and J. W. JOHNSON, *Carbon* **9** (1971) 645.
11. W. S. WILLIAMS, D. A. STEPHANS and R. BACON, *J. Appl. Phys.* **41** (1970) 4893.
12. W. N. REYNOLDS and J. V. SHARP, *Carbon* **12** (1974) 103.
13. D. M. MARSH, *Proc. Roy. Soc.* **A279** (1964) 420.
14. R. BACON, in "Chemistry and Physics of Carbon" (Ed. P. L. Walker) Volume 9, 1973.
15. R. J. DIEFENDORF and E. W. TOKARSKY, AFML-TR-72-133 Part I. Also Ph.D. Thesis (Tokarsky), Rensselaer Polytechnic Inst., 1973.
16. R. J. CHARLES, in "Fracture" (Ed. B. L. Averbach *et al.*) Wiley, 1959.
17. B. L. BUTLER and R. J. DIEFENDORF, Carbon Composite Technology, Proc. 10th Ann. Symp. (New Mexico Section) ASME, Albuquerque 1970, page 107. Also Ph.D. Thesis (Butler), R.P.I., 1969.
18. R. BACON and A. F. SILVAGGI, *Carbon* **9** (1971) 321.
19. A. B. WARDROP and F. W. ADDO-ASHONG, "Proc. Tewksbury Symp. on Fracture" (Ed. C. J. Osborn) 1963, page 183 *et seq.*
20. J. J. GILMAN, "Micromechanics of Flow in Solids", McGraw-Hill (N.Y.) 1969.
21. D. B. FISCHBACH, *J. Chim. Phys.* (No. Spécial) (1969) 121.
22. G. A. COOPER and R. M. MAYER, *J. Mater. Sci.* **6** (1971) 60.

Received 17 June and accepted 27 August 1974.